Nanoscale Metal Oxide Particles/Clusters as Chemical Reagents. Synthesis and Properties of Ultrahigh Surface Area Magnesium Hydroxide and Magnesium Oxide

Suchada Utamapanya, Kenneth J. Klabunde,* and John R. Schlup

Departments of Chemistry and Chemical Engineering, Kansas State University, Manhattan, Kansas 66506

Received August 8, 1990. Revised Manuscript Received October 19, 1990

A modified autoclave hypercritical drying procedure has been used to prepare a hydrated form of MgO from $Mg(OCH_3)_2$ in a methanol–toluene solvent mixture. This material was prepared with 1000 m^2/g surface area and 35-Å crystallite size. Heat treatment of this precursor at 500 °C under vacuum yielded the dehydrated MgO with 500 m^2/g surface area and 45-Å crystallite size. The samples were further characterized by Fourier transform infrared/photoacoustic spectroscopy (FT-IR/PAS), X-ray diffraction, scanning electron microscopy, and chemical analyses. The hydrated precursor contained some residual $-OCH_3$ groups and was much less crystalline in appearance than conventionally prepared $MgO-Mg(OH)_2$ samples. The dehydrated material was free of $-OCH_3$ groups and was made up of much smaller crystallites than conventionally prepared MgO.

Introduction

Clusters, Particles: Highly Divided, High Surface Area Materials. There is currently a revolution in new materials taking place that deals with the synthesis of ultrafine particles (clusters) of inorganic substances.[1] In the solid-state, high surface area, often highly porous materials with individual particle sizes in the 1–100-nm size range are becoming more available. Such materials can range from atoms or single molecules to small clusters of atoms or molecules.[2] These materials are proving to be quite different from bulk, crystalline substances in optical, electrical, magnetic, and physical properties. We call attention to the following quote: "The ability to produce significant quantities of such clusters, and the possibility of the controlled assembly into both noninteracting and interacting arrays, highly porous aggregates, and densely consolidated materials, may offer opportunities for novel properties of these new materials."[1a]

More specifically, ultrafine metal oxide particles have found uses as bactericides, adsorbents, and specifically catalysts.[3,4] One substance in particular has shown great promise as a destructive adsorbent[5] for toxic chemical agents.[6,7] However, the study of nanoscale metal oxides and sulfides has been pursued mainly for their interesting optical and electrical properties.[8–12] Comparativley little has been done regarding their surface chemistry and reactivity.

Nanoscale metal oxide particles will, almost by definition, possess high surface areas, many pores, and coordinatively unsaturated surface cations and anions. They also possess many other types of surface defect sites such as anion and cation vacancies.[13–15] They should possess both acidic and basic sites along with high surface area chemical reaction capacities. Thus, their development as stoichiometric chemical reagents is of interest, and since only surface metal oxide moieties will be reactive, it is important to maximize surface areas, and this is the topic we deal with herein.

Preparative Schemes for Nanoscale Inorganic Materials. There are several approaches to the synthesis of nanoscale inorganic materials, including metal atom clustering in cold solvents,[16] metal ion reduction[17] or precipitation,[18] sometimes reaction in micelle or reverse micelle media,[19] and metal cluster oxidation.[20] A particularly useful approach has been to precipitate metal ions in aqueous media to form a hydroxide gel—the "sol–gel" process.[4] After washing and drying, a fine powder can often be obtained. However, usually the dehydration process of the gel to the oxide causes severe sintering and damage to the pore structure. This is because evaporation

* To whom correspondence should be addressed at the Department of Chemistry.

(1) (a) Andres, R. P.; Averback, R. S.; Brown, W. L.; Brus, L. E.; Goddard, W. A.; Kaldor, A.; Louis, S. G.; Moskovits, M.; Peercy, P. S.; Riley, S. J.; Siegel, R. W.; Spaepan, F.; Wang, Y. *J. Mater. Res.* **1989**, *4*, 704. (b) Pool, R. *Science* **1990**, *248*, 1186. (c) The term cluster has come to mean a small particle of matter made up of about 2–10 000 atoms or molecules. Other terms used over the years are ultrafine particles, highly divided materials, nanophase or nanoscale materials, reactive particles, colloidal particles, and megaclusters.

(2) Klabunde, K. J. *Chemistry of Free Atoms and Particles*; Academic Press: New York, 1980.

(3) Teichner, S. J. *4th Int. Cong. Catal.*; Taniguchi Foundation, Kobe, Japan, Oct 1985; p 59.

(4) Gesser, H. D.; Goswami, P. C. *Chem. Rev.* **1989**, *89*, 765.

(5) By "destructive adsorbent" we mean that during adsorption of a chemical adsorbate on the metal oxide surface, dissociative chemisorption occurs to such an extent that the chemical integrity of the adsorbate molecule is completely destroyed.

(6) Lin, S. T.; Klabunde, K. J. *Langmuir* **1985**, *1*, 600.

(7) Ekerdt, J. G.; Klabunde, K. J.; Shapley, J. R.; White, J. M.; Yates, J. T., Jr. *J. Phys. Chem.* **1988**, *92*, 6182.

(8) Matijevic, E. *Mater. Res. Bull.* **1989**, *Dec*, 18–12.

(9) Fendler, J. H. *Chem. Rev.* **1987**, *87*, 877.

(10) Steigerwald, M.; Alivisotas, A. P.; Gibson, J. M.; Harris, T. D.; Kortan, R.; Mueller, A. J.; Thayer, A. M.; Duncan, T. M.; Douglass, D. C.; Brus, L. E. *J. Am. Chem. Soc.* **1988**, *110*, 3046.

(11) Lianos, P.; Thomas, J. K. *Chem. Phys. Lett.* **1986**, *125*, 299.

(12) Mann, S.; Skavnulis, A. J.; Williams, R. J. P. *J. Chem. Soc., Chem. Commun.* **1979**, 1067.

(13) Klabunde, K. J.; Hoq, M. F.; Mousa, F.; Matsuhashi, H. In *Preparative Chemistry Using Supported Reagents*; Lazslo, P., Ed.; Academic Press: New York, 1987; p 35. This is a review of metal oxides and their physicochemical properties in catalysis and synthesis; see references therein, especially the work of Rees, Wertz, Tanabe, Hattori, Taylor, Sondor, Tench, and others.

(14) Nieves, I.; Klabunde, K. J. *Mater. Chem. Phys.* **1988**, *18*, 485.

(15) (a) Morris, R. M.; Klabunde, K. J. *Inorg. Chem.* **1983**, *22*, 682. (b) Morris, R. M.; Klabunde, K. J. *J. Am. Chem. Soc.* **1983**, *105*, 2633. (c) Klabunde, K. J.; Matsuhashi, H. *J. Am. Chem. Soc.* **1987**, *109*, 1111.

(16) Kerizan, C.; Klabunde, K. J.; Sorensen, C.; Hadjipanayis, G. *Chem. Mater.* **1990**, *2*, 70.

(17) Linnert, T.; Mulvaney, P.; Henglein, A.; Weller, H. *J. Am. Chem. Soc.* **1990**, *112*, 4657.

(18) Sprycha, R.; Matijevic, E. *Langmuir* **1989**, *5*, 479.

(19) Lufimpadio, N.; Nagy, J. B.; Derouane, E. G. In *Surfactants in Solution*; Mittel, K. L., Lindman, B., Eds.; Plenum: New York, 1982; p 1483.

(20) Marquandt, P. *Phys. Lett. A* **1984**, *102*, 365.

0897-4756/91/2803-0175$02.50/0

of the solvent—water—creates a vapor–liquid interface within the capillaries inside the gel network and results in surface tension creating concave menisci inside the network. As the menisci reduce in the gel body, the buildup of tensile force acting on the walls of the pores causes considerable shrinkage due to partial collapse of the gel network. The resultant product, hard, glassy and porous, is generally called a *xerogel*.

To better preserve the texture of the wet gel, the vapor interface inside the pores must be eliminated during the drying process. The most efficient way to eliminate this effect is to remove the liquid within the gel above its critical temperature and pressure (hypercritical) in an autoclave. This approach was first described by Kistler[21] and later improved by Teichner and co-workers,[22,23] and excellent reviews on *aerogel* materials have appeared.[4,24-26]

Metal oxide aerogels are low bulk density materials (sometimes as low as 0.1 g/cm^3), with very large surface areas and large pore volumes. They can be translucent or transparent and generally have extremely low thermal conductivities and fascinating acoustic properties.[4,24-26] Since 1974 they have been used for various applications including as detectors for radiation, superinsulators, solar concentrations, coatings, glass precursors, catalysts, and insecticides.

Interestingly, we have found no reports concerned with aerogels as inorganic reagents for carrying out stoichiometric chemical transformations based on their surface area capacity. This is the area in which we are interested, and herein we report on an improved aerogel procedure for the production of $Mg(OH)_2$ and MgO and some of their interesting properties, while future reports will deal with their utility as chemical reagents.

Results and Discussion

1. General Technique. The approach we and others generally use is to hydrolyze a metal alkoxide in organic media. The hydrolysis and the $M(OH)_x$ polymerization steps are critical and can greatly effect the properties of the gel.[27-29] The degree of hydrolysis, polarity of the M–OR bond, the nature and number of OR groups, temperature, pH, solvent, and dilution can all have an effect.

As hydrolysis takes place, three-dimensional crosslinking prevents crystallization as the gel forms. In practice an alkoxide (single or multicomponent) is mixed in a nonaqueous solvent, sometimes with additives (e.g., acetic acid, ethylene glycol, urea, hydrazine). Water is added, leading to the formation of the sol, a suspension, or dispersion of colloidal particles (1–100 nm) in solution. Destabilization of this sol may be achieved by concentration or further addition of water, giving a gel, an amorphous colloidal/polymeric solid containing a fluid component dispersed in a three-dimensional solid network.

2. Specific Technique. It is known that the morphology of MgO particles is inherited from its precursor species.[15,30] Therefore, to obtain MgO in a highly divided state, a precursor must be synthesized that possesses similar morphology.

Teichner and co-workers have reported the preparation of aerogels of SiO_2, Al_2O_3, TiO_2, ZrO_2, and MgO.[22,23,31] In the case of MgO, they carried out the hydrolysis of magnesium methylate with water in a benzene–methanol solvent mixture and, after autoclave hypercritical drying, obtained magnesia aerogels of 280–407 m^2/g.

We hoped to improve on this surface area. In our modified preparation a solution of magnesium methylate in methanol/toluene was slowly hydrolyzed with water overnight at room temperature. During the process, we observed the formation of a white sol that slowly transformed into a clear gel. The gel was placed in an autoclave of 600-mL capacity, and nitrogen gas was introduced at various pressures (to study the effect of pressure). The autoclave was slowly heated to 265 °C before it was vented in order to evacuate the solvent.[32] The fine powdery white product was obtained in ≈1000 m^2/g form (Table I). From the data in Table I, the effects of a number of variables can be assessed. The autoclave-prepared hydrated samples (AP–MgO–HY) are compared with a conventionally prepared sample.[15a,30] Note the extremely high surface areas for these hydrated samples, more than twice the values reported earlier by Teichner and co-workers[22] and nearly 40 times that of the conventionally prepared samples.

The great improvement in surface area could result from two major factors. First, the use of an excess of toluene solvent could affect the hydrolysis–condensation process. As stated by Hubert-Pfalzgraf, the hydrolysis/condensation/polymerization reactions are governed by several parameters including type of solvent used and dilution.[27] The actual role of each of these parameters is still rather unclear. The interaction between the OH groups and toluene solvent, perhaps, could help protect the gel structure. Likewise, the incorporation of enough hydrophobic solvent may reduce the surface tension at the gas–liquid–pore wall, which is one of the major causes of

Table I. Experimental Conditions and Resultant Surface Areas for MgO Hydrate Aerogels (AP-MgO-HY)[a]

sample	m/s	T, °C	P_{N_2}, psi	S_{BET}, m^2/g	$L_{59(2\theta)}$, Å
AP-MgO-HY					
1	20/50	270	100	843	
2	20/50	263	100	943	72
3	40/100	325	100	867	
4	40/100	325	100	876	
5	40/200	265	100	1104	39
6	20/100	265	100	1028	33
7	20/100	267	100	999	
8	20/100	267	100	926	33
9	20/100	267	600	935	33
10	20/100	265	600	974	
11	20/160	267	100	1003	33
12	20/160	265	100	1005	39
13	20/200	267	100	938	
14	20/200	268	100	891	
15	40/200	268	100	829	42
CP-MgO-HY				28	144

[a] m = 10% magnesium methoxide/methanol solution (grams); s = toluene solvent (grams).

(21) Kistler, S. S. *J. Phys. Chem.* **1932**, *36*, 52.
(22) Teichner, S. J.; Nicolaon, G. A.; Vicarini, M. A.; Gardes, G. E. E. *Adv. Colloid Interface Sci.* **1976**, *5*, 245.
(23) Teichner, S. J. In *Aerogel*; Fricke, J., Ed.; Proceedings of the First International Symposium, Wurzburg, FRG, Sept 23–25, 1985; Springer-Verlag: Berlin, 1986; p 22.
(24) Fricke, J. In ref 23, p 2.
(25) Zarzycki, J.; Woignier, T. In ref 23, p 42.
(26) Schmidt, H.; Scholze, H. In ref 23, p 49.
(27) Hubert-Pfalzgraf, H. J. *New J. Chem.* **1987**, *11*, 663.
(28) Guglielmi, M.; Carturan, G. *J. Non-Cryst. Solids* **1988**, *100*, 16.
(29) Bradley, D. C.; Mehrotra, R. C.; Gaur, D. P. *Metal Alkoxides*; Academic Press: London, 1978.
(30) Morris, R. M. Ph.D. Thesis, University of North Dakota, Grand Forks, ND 1981.
(31) Astier, M.; Bertrand, A.; Bianchi, D.; Chenard, A.; Grades, G. E. E.; Pajonk, G.; Taghavi, M. B.; Teichner, S. J.; Villemin, B. L. In *Preparation of Catalysts*; Delmon, B., et al., Eds.; Elsevier Scientific: New York, 1976; p 315.
(32) The critical temperature of methanol is 241 °C, and that of toluene is 320 °C. Our chosen temperature of 265 °C is based on our finding that it gave the best results and the desire to avoid solvent thermal decomposition. However, 265 °C does not guarantee a true hypercritical condition for the methanol–toluene mixture.

Table II. Elemental Analyses for the MgO Hydrate Aerogels (AP-MgO-HY) and Calculated Empirical Formulas[a]

sample	% Mg	% C	% H	%O[d]	emp formula
AP-MgO-HY[b]					
2	35	9.89	4.41	50.7	$Mg_{1.0}O_{2.2}C_{0.57}H_{3.1}$
5	36	7.70	4.10	52.2	$Mg_{1.0}O_{2.2}C_{0.43}H_{2.7}$
6	31	7.39	3.73	57.9	$Mg_{1.0}O_{2.8}C_{0.48}H_{2.9}$
7	29	8.48	3.02	59.5	$Mg_{1.0}O_{3.1}C_{0.59}H_{2.5}$
8	37	10.7	4.31	48.0	$Mg_{1.0}O_{2.0}C_{0.59}H_{2.8}$
9	34	7.99	3.33	54.7	$Mg_{1.0}O_{2.4}C_{0.48}H_{2.4}$
11	39	6.18	3.54	51.3	$Mg_{1.0}O_{2.0}C_{0.32}H_{2.2}$
12	39	7.37	4.02	49.6	$Mg_{1.0}O_{1.9}C_{0.38}H_{2.5}$
15	37	7.01	3.81	52.2	$Mg_{1.0}O_{2.1}C_{0.38}H_{2.5}$
CP-MgO-HY[c]	39	0.32	2.77	57.9	$Mg_{1.0}O_{2.3}C_{0.01}H_{1.7}$

[a] Note: For pure $Mg(OH)_2$, % Mg = 41.6; % H = 3.43, and % O = 54.9. For pure $Mg(OCH_3)_2$, % Mg = 28.1, % C = 27.8, % H = 6.95, and % O = 37.1. For $HOMgOCH_3$, % Mg = 33.6, % C = 16.6, % H = 5.55, and % O = 44.3. For MgO, % Mg = 60.3, % O = 39.7. [b] Autoclave-prepared samples. [c] Conventionally prepared sample (a standard for comparison). [d] Oxygen % by difference.

the capillary force and stress formation.[33] In our survey experiments, when no toluene was used (only methanol–water) products with surface area of ≈400 m^2/g were obtained. In the case of some toluene solvent, i.e. methoxide solution/toluene (m/s) = 50/100, the surface area increased to ≈800–900 m^2/g. The use of more toluene (m/s = 20/100) gave further improvement to ≈1000 m^2/g. A larger excess of toluene solvent, i.e., m/s = 20/160 and 20/200, did not further improve the surface area of the final product. It seems that there is a minimal amount of organic solvent required for an optimal specific surface area.

Second, the introduction of nitrogen gas just prior to autoclave treatment could have an effect toward minimizing shrinkage of the gel during the drying process. Mulder and van Lierop[34] have reported such findings with autoclave-treated silica gels. The reason for this effect probably is to suppress bubble formation and boiling while heating to the critical temperature of the solvent. In our experiments, a pressure of ≈100 psi (1.8 bar, 1.8×10^5 Pa) appears optimum. Application of higher pressure such as 600 psi (40.8 bar, 40.8×10^5 Pa) did not improve the surface area of the product magnesium oxide hydrate.

3. Characterization of Magnesium Oxide Hydrate (AP-MgO-HY). Nine representative autoclave-prepared samples were further characterized. Interestingly, chemical analysis data showed that the dry samples contained 6–10 wt % C and 4 wt % H (Table II). Such high residual C and H contents for aerogels were also encountered by Teicher and co-workers[22] working with silica. They also reported that alumina and titania aerogels contained 4–5 wt % C. Since adequate amounts of water were added to completely hydrolyze M–OR groups, it seems likely that esterification of O–H groups by alcoholic solvent was encouraged by the autoclave treatment conditions:[22,34]

$$-OMgOH + CH_3OH \rightleftarrows -OMg-OCH_3 + H_2O$$

Many AP-MgO-HY samples were examined by Fourier transform infrared/photoacoustic spectroscopy (FT-IR/PAS) and powder X-ray diffraction (XRD). Figure 1 shows a typical spectrum (AP-MgO-HY-8 (a), Table I) for an autoclave-prepared MgO hydrate. Note bands at 1100, 1450, 2792, 2837, and 2911 cm^{-1}, which are all indicative of the presence of $-OCH_3$ groups. The band at 3740 cm^{-1} indicates bulk –OH. This sample has the highest

(33) Schmidt, H. *J. Non-Cryst. Solids* **1988**, *100*, 51.
(34) Mulder, C. A. M.; van Lierop, J. G. In ref 23, p 68.

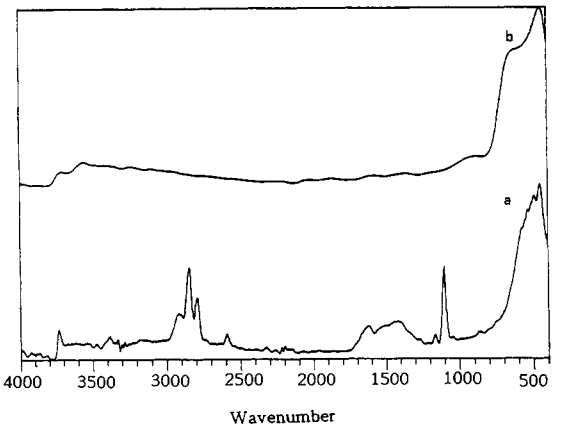

Figure 1. FT-IR/PAS spectra of (a) AP-MgO-HY-8 (4 cm^{-1}, 256 scans) and (b) AP-MgO-8 samples (4 cm^{-1}, 64 scans). The vertical axis is percent absorbance.

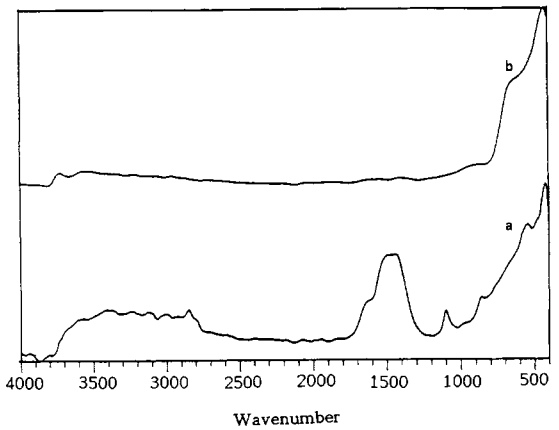

Figure 2. FT-IR/PAS spectra of (a) AP-MgO-HY-6 (4 cm^{-1}, 256 scans) and (b) AP-MgO-6 samples (4 cm^{-1}, 64 scans). The vertical axis is percent absorbance.

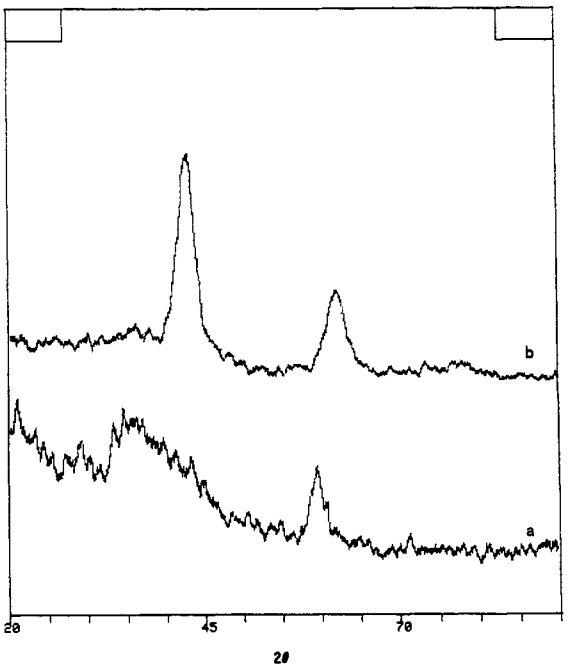

Figure 3. XRD spectra of (a) AP-MgO-HY-6 and (b) AP-MgO-6 samples.

C, H content (Table II). If we look at sample 6, with a lower C, H content, the consequent lower concentration of $-OCH_3$ groups is evident in the FT-IR/PAS spectrum (Figure 2).

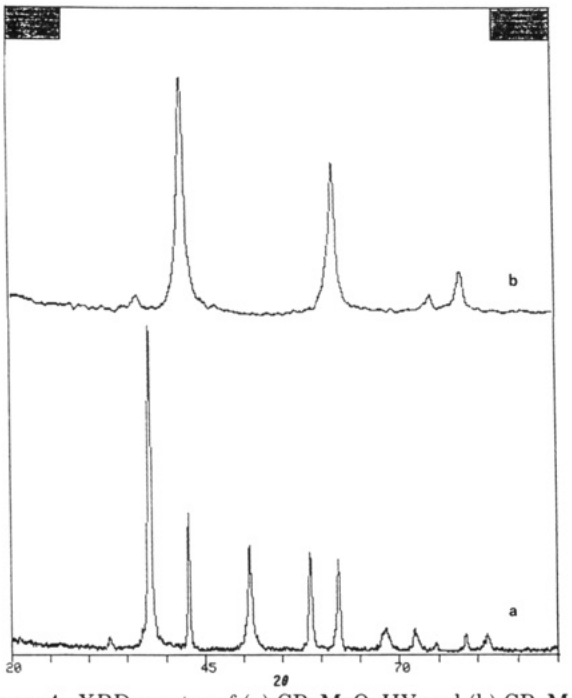

Figure 4. XRD spectra of (a) CP–MgO–HY and (b) CP–MgO samples.

Powder XRD spectra for all the AP samples were similar. Figure 3 illustrates that for the hydrated sample AP–MgO–HY–6 fresh from the autoclave with no heat treatment. Obviously the peaks are very broad, indicative of the expected small particular size. For comparison, Figure 4 shows the XRD pattern for our conventionally prepared sample CP–MgO–HY, which fits brucite (mainly) with some crystalline MgO also present.

The crystallites sizes of the AP–MgO–HY samples were calculated from the line broadening of the peak at 59 (2θ), using the Scherrer equation; $L_{59(2\theta)}$ in Table I. Note that there is reasonably good agreement between surface area measurements and crystallite size calculations from XRD.

Table III. Surface Areas and Crystallite Sizes of Nanoscale Dehydrated MgO Samples (AP-MgO)[a,b]

sample	S, m^2/g	$L_{62(2\theta)}$, Å
AP–MgO		
2	343	40
5	406	40
6	463	36
7	408	44
8	485	73
9	270	44
11	522	49
12	464	40
15	471	40
CP–MgO	219	88

[a] AP–MgO samples obtained from AP–MgO–HY samples by heating under vacuum slowly to 500 °C (see Experimental Section). [b] Usually about a 40% weight loss took place during the heat-treatment process.

We have seen that spectra and physical data clearly differentiate between the AP–MgO–HY and CP–MgO–HY samples. This clear difference can also be observed in the electron microscope. The CP–MgO–HY (Figure 5) SEM photograph clearly shows beautiful hexagonal platelets of brucite while the AP–MgO–HY samples show no clear crystal structure (Figure 6).

Nanoscale MgO. High-temperature treatment (500 °C) of the hydrated MgO yields MgO. (We chose a 500 °C treatment based on our earlier results showing that this was often the optimum temperature with regard to preserving surface area and surface reactivity while still being hot enough to eliminate water and most surface –OH groups.)[13–15,30] This step is crucial and must be done carefully in order to preserve the ultrahigh surface area. Very slow heating under a good dynamic vacuum are usually the best conditions, although small samples have been heat treated successfully under flowing Ar or N_2.[15c] Table III summarizes the surface areas (BET) and crystallite sizes (XRD) obtained after heating the AP–MgO–HY samples to dehydrate them to AP–MgO. For comparison a conventionally prepared sample is also shown.

Figure 5. SEM pictures of a CP–MgO–HY sample.

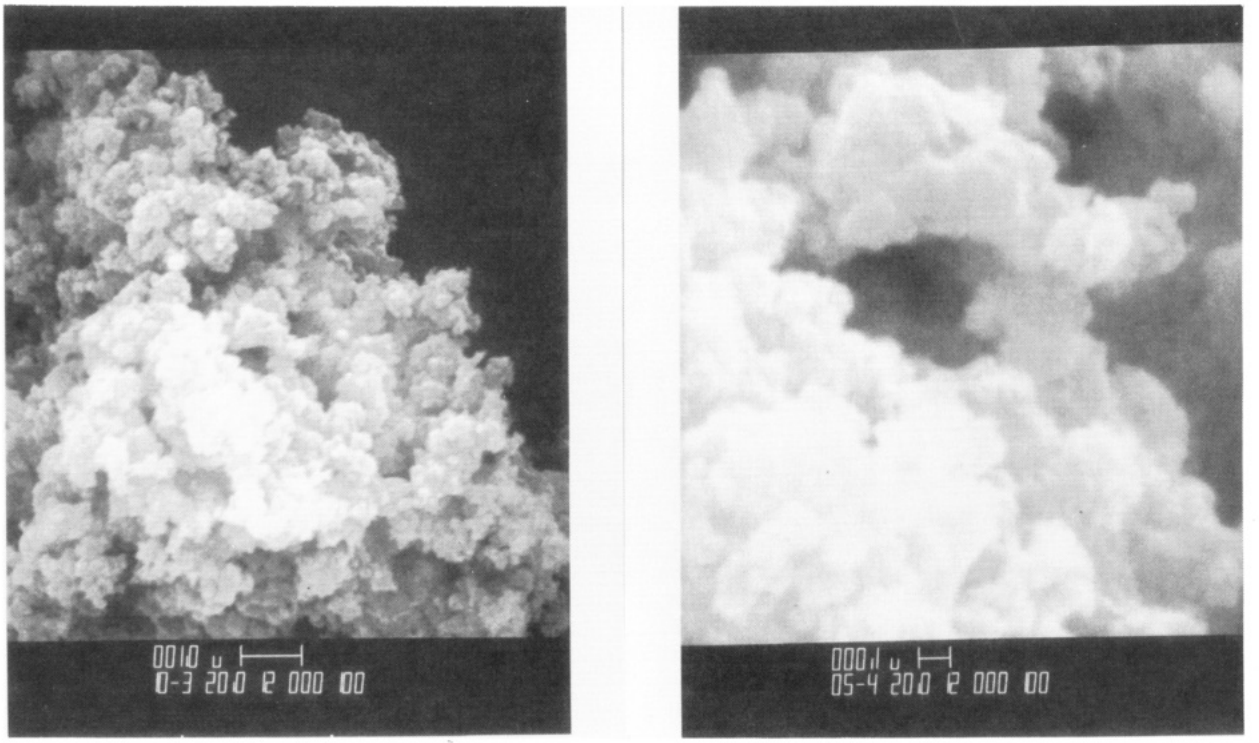

Figure 6. SEM pictures of a AP–MgO–HY–5 sample.

It is interesting to compare the data in Tables I and III. Note that the autoclave-prepared samples lost about one-half their surface area upon dehydration. On the other hand, the CP–MgO–HY samples surface area *increased* dramatically upon heat treatment, which indicates that larger crystals actually form a pore structure upon dehydration. These results agree with those reported by Anderson and Horlock, where they heat treated 30 m^2/g $Mg(OH)_2$ (brucite) and obtained 210 m^2/g MgO.[35] Thus, in the final stages of $Mg(OH)_2$ decomposition to MgO and H_2O, crystallization takes place, but crystallite sintering does not take place if the hot steam is removed quickly.

Returning to autoclave-prepared aerogel samples, Teichner and co-workers[22] reported that thermal treatment of alumina aerogels in air at 600 °C caused a larger decrease in surface area, but similar treatment in vacuum had no radical effect on textural characteristics. Air heat treatment of zirconia aerogel was also more detrimental than vacuum treatment. For example, 400 °C in air caused the zirconia aerogel to rapidly lose surface area, while vacuum treatment preserved the texture up to 500 °C. However, vacuum treatment at 600 °C caused a surface area loss from 322 to 84 m^2/g.

Our work with MgO aerogels shows similar tendencies. Surface areas did decrease substantially upon dehydration under vacuum. However, small crystallites are preserved, and even with the surface area decreases we still were able to routinely obtain MgO samples of 400–500 m^2/g, which is a great improvement over conventionally prepared samples. Figures 3 and 4 show the XRD patterns for the AP–MgO and CP–MgO samples.

Chemical analyses of AP–MgO samples indicated that carbon and hydrogen content has been reduced to low levels (~0.2% C and 0.2% H). The FT-IR/PAS spectra of these samples are shown in Figures 1 and 2, confirming that organic OCH_3 groups have been lost by heat treating under vacuum and very little –OH remains.

(35) Anderson, P. J.; Horlock, R. F. *Trans. Faraday Soc.* **1962**, *58*, 1993.

Particle morphology of the heat treated samples was observed by SEM (Figures 7 and 8). As found for the hydrated samples, a more crystalline morphology was observed for the CP–MgO samples, while the AP–MgO appeared almost amorphous.

Conclusions

Nanoscale hydrated MgO precursors (mainly $Mg(OH)_2$ with some $OMgOCH_3$ residues) with surface areas of ≈1000 m^2/g were prepared by a modified autoclave aerogel preparation. Heat treatment of the hydrated precursors yielded the desired MgO product with surface areas of ≈500 m^2/g. These results demonstrate a substantial improvement compared with conventionally prepared samples of MgO from $Mg(OH)_2$, $MgCO_3$, or $Mg(NO_3)_2$. Morphology as determined by SEM indicated a rather crystalline nature for the conventionally prepared samples while the autoclave-prepared samples appeared to be made up of much smaller crystallites.

High surface area, amorphous materials tend to possess higher surface concentrations of reactive defect sites, allowing more interesting properties as base catalysts and adsorbents. With the availability of these new high surface area materials, such improved performance has been realized. Details concerning this surface chemistry will be reported later.

Experimental Section

A. Preparation of the Highly Divided MgO Precursors. Preparation of 10% magnesium methoxide in methanol solution: We employed the reaction of magnesium ribbon with analytical grade methanol at room temperature. The Mg ribbon surface was rubbed with sandpaper, followed with acetone-wet Kimwipe, and cut into small peieces (about 0.5–1 in.) before use. To prevent the hydrolysis of the resulting methoxide product by atmospheric moisture, the reaction was carried out under a slow flow of N_2 gas. Thus 5 g of Mg (0.20 mol) was stirred with 205 mL of methanol in a 500-mL round-bottom flask equipped with the N_2 gas inlet and outlet at room temperature. The reaction between Mg metal and methanol occurred very slowly and could be observed by formation of H_2 gas bubbles inside the reaction

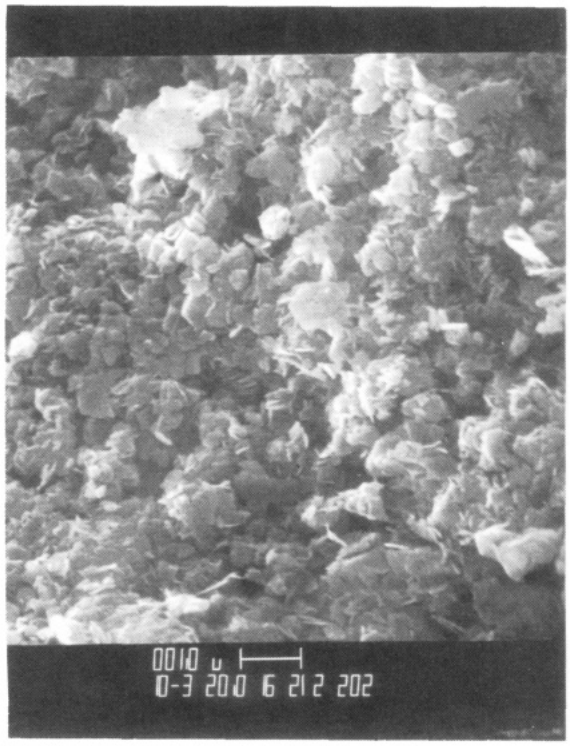

Figure 7. SEM picture of a CP–MgO sample.

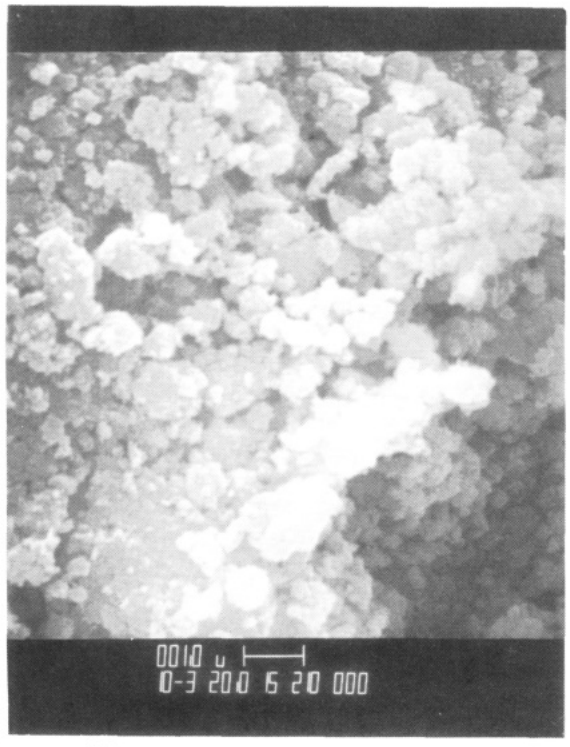

Figure 8. SEM picture of a AP–MgO–5 sample.

flask. The reaction mixture was stirred overnight, and it was ready for use after all of the Mg metal had reacted. The solution was stored in the reaction flask for future use.

Hydrolysis of magnesium methoxide solution: Portions of magnesium methoxide in methanol solution (10% by weight) were placed in a 400-mL beaker (either 20 or 40 g of solution). Toluene solvent was added to make the desired dilution as shown in Table I. From a syringe, triply distilled water (0.9 or 1.8 mL) was slowly added into the stirring solution. A white cloudy precipitate was observed upon the addition of each drop of water. After a few minutes, the mixture became a clear, syruplike solution. To minimize the evaporation of organic solvent, the beaker top was covered with aluminum foil. The reaction was checked a few hours later by adding a drop of water. If a large amount

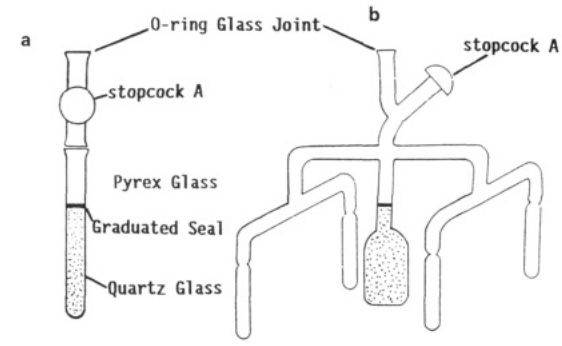

Figure 9. Sample cells for heat treatment experiments (a) for small samples and (b) for large samples.

of the white precipitate was formed, a few more drops of water were added into the reaction mixture. The resulting mixture was stirred overnight to ensure the completion of the hydrolysis.

Autoclave treatment procedure: The hydroxide gel solution was transferred into the glass-lined 600-mL capacity Parr minireactor. After being flushed with a flow of N_2 gas, the reactor was then pressurized with N_2 gas to obtain the desired pressure of 100 or 600 psi. The reactor was slowly heated from room temperature to the required set point at a rate of 1 °C/min by the PID controller (about 4 h). The temperature was allowed to equilibrate at the set point for 10 min before the reactor was vented to release the pressure, which took about 0.5–1 min. The reactor was immediately removed from the heater and then flushed with N_2 gas for about 5–10 min. After it was allowed to cool to room temperature, the product was removed from the reactor and was further dried in an oven at 120 °C for a few hours. The final product was stored in a bottle for future use.

Note: During the heating process, the pressure inside the reactor rose slowly. The final pressure at the set point was dependent upon experimental conditions, such as the initial N_2 pressure and the final set point temperature. For a typical condition such as 20/100 or 40/200 solution of methoxide/toluene with 100 psi of N_2, the pressure slowly increased to about 600–900 psi at the set point temperature of 265 °C. With the initial pressure of 600 psi, a final pressure of 1560–1580 psi was reached at 265 °C. For the 40/100 solution with of 100 psi of N_2, a pressure as high as 1350–1500 psi can be expected at 320 °C.

B. Heat Treatment (Thermal Activation) Procedure. The hydrated MgO (about 50–100 mg) obtained from the autoclave/oven drying procedure was evacuated in a quartz tube cell (Figure 9) to below 5 mTorr before the heating process was started. The cell was heated (under dynamic vacuum) by using a furnace controlled by the PID temperature controller with ramp and soak capability. The ramp and soak heating condition for the experiments was the following: ramp from room temperature to 220 °C at 1 °C/min; soak at 220 °C for 5 h; ramp from 220 to 500 °C at 1 °C/min; soak at 500 °C for 5 h.

About 18 h was required for the heat treatment of a sample. After the heat treatment, the sample was allowed to cool to room temperature (usually about 3 h). The sample was weighed and then stored under N_2. This heating process caused a 40% weight loss overall. Theory predicts a 31% loss for $Mg(OH)_2 \rightarrow MgO$. The larger than predicted weight loss indicates that some organic residue is also evolved (OCH_3 groups) and that mechanical losses are also significant.

A special cell (Figure 9b) was designed to accommodate the activation of a large sample for different measurements (as needed for surface area, chemical analysis, FT-IR/PAS, XRD, and SEM) and 150–200 mg of sample could be activated in the cell under the same conditions as described above. After activation, stopcock A was tightly closed and the sample cell was isolated from the vacuum line. The sample was transferred into a different section of the sidearm tubes as needed before each tube was carefully flame sealed. The sample tubes were kept for future experiments and removed just before each measurement.

C. Surface Area Measurement. The surface area of the sample was determined by the Micromeritics Flowsorb II 2300 instrument, equipped with a Dual Channel System Unit (900 Series, Sierra Instruments).

The surface area of solids was measured with the FlowSorb 2300 by determining the quantity of a gas that adsorbs as a single layer of molecules (monomolecular layer) on a sample. This adsorption is done at or near the boiling point of the adsorbate gas. This area of the sample was directly calculated from the number of adsorbed molecules, which was derived from the gas quantity, and the area occupied by each. Nitrogen in helium (30/70) with liquid nitrogen as the cold bath provides the most frequently used conditions. The dual-channel system unit is a mass flow controller that measures and automatically controls two gas streams as required for gas blending. A gas composition of approximately 30% N_2 and 70% He used for all the surface area measurement was obtained from the dual-channel system unit.

Calibration of the FlowSorb II for Single-Point Surface Area Measurement. Calibration of the FlowSorb II was accomplished by injecting a precise volume of N_2 gas and adjusting the instrument to indicate the surface area value as calculated by using the following equation:

$$S = \upsilon \frac{273.2}{T_R} \frac{P}{760} \frac{6.023 \times 10^{23} \times 16.2 \times 10^{-20}}{22.414 \times 1000} \left(1 - \frac{(\%N/100)P}{P_s}\right)$$

where S = surface area (m^2), υ = volume of gas injected (mL), (T_R) = room temperature (°C), P = atmospheric pressure (mmHg), and P_s = saturation pressure of liquid nitrogen (775 mmHg for pure liquid nitrogen).

Under our experimental conditions (1 mL of N_2 gas injected at 22 °C and 760 mmHg), the instrument must be calibrated to produce an indicated surface area of 2.84 m^2.

D. Chemical Analysis. The Mg analysis was carried out by Frank Padula, the University Analytical Laboratory, Kansas State University. The following procedures were carried out.

The sample was dissolved with high-purity $HCl/HNO_3/HF$. The HCl was added first as not to form hardened nitrates. HNO_3 was added next, following by a trace of HF. An acid blank was carried through at all times, and all standards were made up in the same matrix of acid proportions. The sample was analyzed by direct current plasma (DCP) emission spectrometry using a Beckman/Spectrometrics ARL, DCP III modified to a V with an analytical data manager (ADAM) system. Sample and standard were made or diluted by weight and ADAM calculated the results (w/w %).

The carbon and hydrogen content in all samples was analyzed by Dr. Gregory M. Dabkowski of the Microlytics, PO Box 199, South Deerfield, MA 01373.

E. Spectroscopic Measurements. Fourier-transform infrared/photoacoustic spectroscopy: The FT-IR/PAS experiments were carried out by using a MTEC Model 100 photoacoustic cell and a Mattson-CYGNUS 100 FT-IR spectrometer. The instrument utilized a high-temperature ceramic source and a germanium-coated KBr beam splitter. The spectra were obtained with resolutions of 4 or 8 cm^{-1} and 64 or 128 scans (mirror velocity of 0.12 cm/s). Carbon black was used as the reference material.

X-ray Diffraction: For the XRD experiments, the samples were loaded onto the cell provided with the spectrometer (Sintag-XDS-2000). The activated sample tubes were broken off just before each measurement and were immediately loaded on to the cell. The contact time to the atmospheric environment was kept to a minimum (about 2–3 min). The spectrometer was set at 40 kV and 45 mA and typical scans were from 20 to 90 (2θ) at 2°/min.

Scanning electron microscopy: The hydrated MgO sample was held onto a small piece of sticky transparent tape on top of the specimen mount stub for the electron microscope study. For the heat-treated (dehydrated) sample, the sample loading was carried out inside a N_2 bag and was kept in a plastic box inside a desiccator during the period before the gold-coating operation. A gold film of about 30-nm thickness was obtained from a sputtering coater with four layers of 10-s coating time. The SEM pictures were taken by using the ETEC (Autoscan Model) spectrometer by Larry Sieb of the Chemical Engineering Department, Kansas State University.

F. Materials and Equipment. Chemicals: Mg ribbon, Fisher Scientific Company; 5–10% magnesium methoxide in methanol solution, Pfaltz & Bauer Inc., Cat No. 00480; methanol, spectroscopic grade, Fisher Scientific Co.; toluene, reagent grade, Fisher Scientific Co.

Equipment: bench top minireactor, Parr Co., Model 4563-SS-P-115-VS-2000-4843, 600-mL capacity, T316 stainless stell bomb with packed gland, variable-speed stirrer, 2000 psi pressure gage, and PID programmable controller; x-ray diffraction spectrometer, Scintag-XDS-2000; scanning electron microscope, ETEC-Autoscan.

Appendix: Calculation of Crystallite Size of Powder Samples from the X-ray Line Broadening

The crystallite size of a power sample can be estimated from the X-ray broadening by using the well-known Scherrer equation:[36–38]

$$B(2\theta) = \frac{0.89\lambda}{L \cos \theta}$$

where $B(2\theta)$ is the width of the X-ray pattern line at half peak-height in radians, λ is the wavelength of the X-ray (1.540 51 Å for the Cu K2α), θ is the angle between incident and diffracted beams in degrees, and L is the crystallite size of the powder samples in angstroms.

Acknowledgment. The financial support of the Army Research Office is acknowledged with gratitude. Partial support came from the U.S. Environmental Protection Agency and the U.S. Department of Energy, through the Hazardous Substance Research Center headquarters at Kansas State University. The findings have not been subjected to EPA review and may not reflect the view of the Agency.

Registry No. MgO, 1309-48-4; $Mg(OCH_3)_2$, 27428-49-5; $Mg(OH)_2$, 1309-42-8.

(36) Mikhail, R. S.; Robens, E. *Microstructure and Thermal Analysis of Solid Surfaces*; Wiley: Chichester, 1983; Part 1.
(37) Innes, W. B. In *Experimental Methods in Catalytic Research*; Anderson, R. B., Ed.; Academic Press: New York, 1968; p 44.
(38) Warren, B. E. *X-ray Diffraction*; Addision-Wesley: Reading, MA, 1969; p 21.